JOURNAL OF THEORETICAL AND APPLIED MECHANICS
52, 3, pp. 629-639, Warsaw 2014

ANALYSIS OF THE DYNAMICS AND CONTROL OF THE MODIFIED OPTICAL TARGET SEEKER USED IN ANTI-AIRCRAFT ROCKET MISSILES

Daniel Gapiński, Izabela Krzysztofik, Zbigniew Koruba
Kielce University of Technology, Faculty of Mechatronics and Machine Design, Kielce, Poland
e-mail: tu_daniel_kielce@wp.pl; pssik@tu.kielce.pl; ksmzko@tu.kielce.pl

The paper presents the concept of programmed control of the designed optical target seeker in the phase of searching the air space. The controlling of the programmed movements of the seeker axis has been developed with simultaneous consideration of the process of scanning of the air space by an optoelectronic system of the device. Numerical analysis of the dynamics of the proposed optical scanning seeker as well as the analysis of selection of velocity and suitable trajectories of the displacement of its axis were conducted. The results were presented in a graphical form.

Keywords: self-guidance, dynamics and control, target seeker, rocket missile

1. Introduction

Optical scanning heads of self-guided rocket missiles are devices requiring high accuracy and precision of making (Awrejcewicz and Koruba, 2012; Moir and Seabridge, 2006; Siouris, 2004).

Structural solutions of those devices are constantly improved because detection and determination of the location of faster and faster moving air targets in real conditions is additionally hindered by various thermal disruptions (Yanushevsky, 2008). In connection with the above, optical systems and structural solutions of those devices are still improved what is proven by the most recent European and American patents published in the years 2010-2012 (Barenz *et al.*, 2012; Kröner, 2012; Rueger and Zoz, 2012; Shaffer, 2011; Wellman *et al.*, 2010, Wild and Leavy, 2012). The possibility of using innovative structural solutions is considered, and the optimization of the process of scanning (searching) of the air space by the designed scanning seeker is presented in the paper. Innovation and the principle of operation have been presented in the patent description (Gapiński, 2005).

The design of the developed scanning seeker (Gapiński, 2005), including the most significant constituents, is shown in Fig. 1.

- The gyroscope rotor consists of the following elements presented in Fig. 1:

  2 – primary mirror, 3 – secondary mirror guard, 4 – adjustable secondary mirror, 5 – secondary mirror roller, 6 – pattern board with electromagnet, 8 – retaining ring, 9 – fastening lid, 10 – body of mechanical gyroscope, 11 – corrective lens system, 12 – permanent magnet of driving motor, 14 – additional movable mirror, 18 – gear transmission, 19 – snap ring, 20 – bearing, 21 – two spacer bushings.
- The complete inner housing consists of:

  1 – coil of driving motor, 15 – electric motor controlling inner housing, 13 – two infrared radiation receivers, 17 – pattern board with electromagnet, 24 – fastening board, 25 – two fibre-optic gyroscopes, 26 – inner housing, 29 – bearing fastening, 31 – moving axis, 32 – bearing.

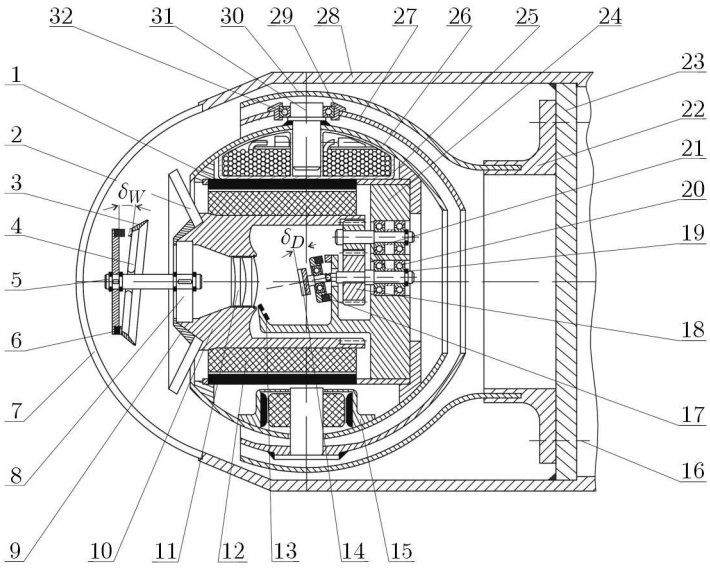

Fig. 1. Structure of the modified scanning seeker

- The complete outer housing consists of:

  15 – electric motor controlling outer housing, 27 – outer housing, 29 – bearing fastening, 31 – moving axis, 32 – bearing.

2. Model of the seeker movement

Figure 2 shows a diagram of the seeker, including the adopted systems of coordinates as well as markings of individual angles of rotations of the respective systems in relation one to another.

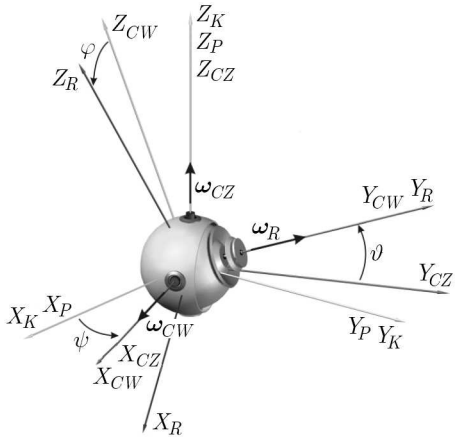

Fig. 2. The diagram of the seeker, including the adopted systems of coordinates

A gyroscope movement can take place under the influence of moments of external forces M_Z and M_W generated by controlling motors (15) as well as angular movements of the rocket missile deck determined with the use of angular velocities ω_{x_P}, ω_{y_P}, ω_{z_P} causing its rotation around individual axes of the system $OX_PY_PZ_P$ with the respective angles α_{x_P}, α_{y_P} and α_{z_P}.

The following systems of coordinates (Awrejcewicz and Koruba, 2012; Baranowski, 2013; Krzysztofik, 2012) were introduced:

$OX_KY_KZ_K$ – system of coordinates connected with the direction set in space,

$OX_PY_PZ_P$ – moving coordinate system connected with the missile,

$OX_{CZ}Y_{CZ}Z_{CZ}$ – moving coordinate system connected with the outer housing,
$OX_{CW}Y_{CW}Z_{CW}$ – moving coordinate system connected with the inner housing,
$OX_RY_RZ_R$ – moving coordinate system connected with the rotor.

The following markings of angles of rotation and the order of measuring them were adopted:
ψ – angle of rotation $OX_{CZ}Y_{CZ}Z_{CZ}$ in relation to $OX_PY_PZ_P$ around axis Z_{CZ},
ϑ – angle of rotation $OX_{CW}Y_{CW}Z_{CW}$ in relation to $OX_{CZ}Y_{CZ}Z_{CZ}$ around axis X_{CW},
ϕ – angle of rotation $OX_RY_RZ_R$ in relation to $OX_{CW}Y_{CW}Z_{CW}$ around axis Y_R.

Hence, the location of gyroscope rotor in relation to the system $OX_PY_PZ_P$ is determined with the use of three angles: ψ, ϑ, ϕ.

As given quantities the following were adopted:

1. $J_{x_{CZ}}, J_{y_{CZ}}, J_{z_{CZ}}$ – moments of complete inertia of the outer housing,
2. $J_{x_{CW}}, J_{y_{CW}}, J_{z_{CW}}$ – moments of complete inertia of the inner housing,
3. $J_{x_R}, J_{y_R}, J_{z_R}$ – moments of inertia of the rotor,
4. $\boldsymbol{\omega}_P(\omega_{x_P}, \omega_{y_P}, \omega_{z_P})$ – missile angular velocity;
5. $\mathbf{M}_Z$ – moment of missile forces interacting with the outer housing,
6. $\mathbf{M}_W$ – moment of forces of the outer housing interacting with the inner housing,
7. $\mathbf{M}_R$ – moment of forces of the inner housing interacting with the rotor,
8. $\mathbf{M}_{TR}$ – moment of friction forces in rotor bearings and aerodynamic resistance,
9. $\mathbf{M}_{TW}, \mathbf{M}_{TZ}$ – moments of friction forces in the bearings of the inner and outer housing, respectively.

The equations of seeker (gyroscope) motion have been introduced with the use of Lagrange equations of the II-nd kind (Awrejcewicz and Koruba, 2012; Baranowski, 2013; Krzysztofik, 2012)

$$\begin{aligned}
&J_{z_{CZ}}\frac{d}{dt}\omega_{z_{CZ}} + J_{y_{CW}}\frac{d}{dt}(\omega_{y_{CW}}\sin\vartheta) + J_{z_{CW}}\frac{d}{dt}(\omega_{z_{CW}}\cos\vartheta) + J_{y_R}\frac{d}{dt}(\omega_{y_R}\sin\vartheta)\\
&\quad + J_{z_R}\frac{d}{dt}(\omega_{z_{CW}}\cos\vartheta) - (J_{x_{CZ}} - J_{y_{CZ}})\omega_{x_{CZ}}\omega_{y_{CZ}} - (J_{x_{CW}} + J_{x_R})\omega_{x_{CW}}\omega_{y_{CZ}}\\
&\quad + J_{y_{CW}}\omega_{y_{CW}}\omega_{x_{CZ}}\cos\vartheta - (J_{z_{CW}} + J_{z_R})\omega_{z_{CW}}\omega_{x_{CZ}}\sin\vartheta + J_{y_R}\omega_{y_R}\omega_{x_{CZ}}\cos\vartheta\\
&\quad = M_Z - M_{TZ}\\
&J_{x_{CW}}\frac{d}{dt}\omega_{x_{CW}} + J_{x_R}\frac{d}{dt}\omega_{x_{CW}} - (J_{y_{CW}} - J_{z_{CW}} - J_{z_R})\omega_{y_{CW}}\omega_{z_{CW}} - J_{y_R}\omega_{y_R}\omega_{z_{CW}}\\
&\quad = M_W - M_{TW}\\
&J_{y_R}\frac{d}{dt}(\omega_{y_{CW}} + \dot{\phi}) = M_R - M_{TR}
\end{aligned} \tag{2.1}$$

where

$$\begin{aligned}
&\omega_{x_{CZ}} = \omega_{x_P}\cos\psi + \omega_{y_P}\sin\psi && \omega_{y_{CZ}} = -\omega_{x_P}\sin\psi + \omega_{y_P}\cos\psi\\
&\omega_{z_{CZ}} = \dot{\psi} + \omega_{z_P} && \omega_{x_{CW}} = \omega_{x_{CZ}} + \dot{\vartheta}\\
&\omega_{y_{CW}} = \omega_{y_{CZ}}\cos\vartheta + \omega_{z_{CZ}}\sin\vartheta && \omega_{z_{CW}} = -\omega_{y_{CZ}}\sin\vartheta + \omega_{z_{CZ}}\cos\vartheta\\
&M_{TW} = c_w\dot{\vartheta} && M_{TZ} = c_z\dot{\psi}
\end{aligned}$$

and c_w is the friction coefficient in the bearing of the inner housing, c_z – friction coefficient in the bearing of the outer housing.

We assume that $M_R = M_{TR}$, then $\omega_{y_R} = \omega_R = n = \text{const}$ (n is the angular velocity of the rotor) and motion of the seeker axis is governed by equations $(2.1)_{1,2}$.

3. Controlling motion of the seeker axis

On contemporary battlefields, the precise aiming of a missile at a moving air target is undoubtedly a difficult thing to accomplish. The scanning seeker proposed in the paper will allow one to aim the missile only in the direction of the foreseen location of the target. The optical axis of the seeker performs programmed movements (e.g. in a circle) and, simultaneously, the system of mirrors scans the surface on an n-leaved rosette with the so called big scanning angle. It increases the area of searching and, with a suitable selection of velocity of the programmed movement of the seeker axis, gives satisfactorily dense scanning of space. At the moment of intercepting the target by the scanning seeker, the angles by which the seeker axis is to be moved so that it overlapped with the line of sight (LOS) are determined. It is still the programmed control which can be carried out, e.g. in a straight line. During that control phase, the angles ϑ_Z, ψ_Z determine the set (desired) programmed movement which should be made by the axis of the scanning seeker so that it overlapped with LOS. After intercepting the target and the programmed presentation of the seeker axis on LOS, there is the second phase consisting in the tracking of the target. During that phase, the rocket missile is launched, while the angles ϑ_Z, ψ_Z are determined systematically by the target seeker optical system. At the moment of finishing the operation by the missile start motor (stabilisation of the trajectory of the missile flight), there appears a decrease in the angles δ_W and δ_D what causes the narrowing down of the area of the scanned space. The angles δ_W and δ_D are inclination angles of the primary and secondary mirror respectively in relation to the seeker axis. They are shown in Fig. 1. The selection of those angles is presented in the paper by Gapiński (2013).

The passing of the seeker from the searching mode to the tracking mode, and the simultaneous interaction of the rocket missile deck adversely affect the long maintaining with a sufficient precision the programmed movement and the tracking through its axis. We eliminate by that the suitably chosen correction system.

The control law for the axis of the scanning seeker (Awrejcewicz and Koruba, 2012; Blakelock, 1991; Ładyżyńska-Kozdraś, 2009) can be written in the following way

$$M_W = \Pi(t_o, t_w)M_W^p(t) + \Pi(t_s, t_k)M_W^s \qquad M_Z = \Pi(t_o, t_w)M_Z^p(t) + \Pi(t_s, t_k)M_Z^s \tag{3.1}$$

where M_W^p, M_Z^p are program controls for the seeker axis, M_W^s, M_Z^s – tracking controls for the seeker axis, $\Pi(t_o, t_w)$, $\Pi(t_s, t_k)$ – functions of rectangular impulse, t_0 – moment of the beginning of the scanning of space, t_w – moment of detecting the target, t_s – moment of the beginning of the tracking of the target $(t_s = t_w)$, t_k – moment of the finishing of the process of self-guidance.

The program controls M_W^p, M_Z^p can be determined from the dependence (Koruba *et al.*, 2010)

$$\begin{aligned} M_W^p &= -k_w(\vartheta - \vartheta_Z) + k_z(\psi - \psi_Z) - h_z(\dot{\vartheta} - \dot{\vartheta}_Z) \\ M_Z^p &= -k_z(\vartheta - \vartheta_Z) - k_w(\psi - \psi_Z) - h_z(\dot{\psi} - \dot{\psi}_Z) \end{aligned} \tag{3.2}$$

where ϑ, ψ are real angles determining the location of the seeker axis in space, ϑ_Z, ψ_Z – set angles determining the location of the seeker axis in space, k_w, k_z, h_z – controller coefficients.

The tracking controls M_W^s, M_Z^s can be determined from the dependence (Koruba *et al.*, 2010)

$$\begin{aligned} M_W^s &= -k_w(\vartheta - \varepsilon) + k_z(\psi - \sigma) - h_z(\dot{\vartheta} - \dot{\varepsilon}) \\ M_Z^s &= -k_z(\vartheta - \varepsilon) - k_w(\psi - \sigma) - h_z(\dot{\psi} - \dot{\sigma}) \end{aligned} \tag{3.3}$$

The angles ε, σ are angles determining the current location of LOS in space, determined systematically through the optoelectronic system of the scanning seeker.

4. Results

Numerical research was conducted for the designed scanning seeker intended for the close-range surface-to-air rocket missiles.

4.1. Parameters of the seeker

The moments of inertia of individual elements of the seeker have been calculated in relation to respective axes of the adopted systems of coordinates (shown in Fig. 2). The beginnings of all systems of coordinates overlap and are at the intersection of the axis of rotation of the outer housing with the axis of rotation of the inner housing of the seeker. The maximum torques of individual motors controlling the outer and inner housing have been determined based on the previous analysis of the designed seeker dynamics. The selection of a suitable gear ratio (18) results from the analysis of the cooperation of individual seeker mirrors.

- Moments of inertia of the rotor are:

  $J_{x_R} = 0.00114143\,\mathrm{kg\,m^2},\ J_{y_R} = 0.00157911\,\mathrm{kg\,m^2},\ J_{z_R} = 0.00158234\,\mathrm{kg\,m^2}$
- Moments of complete inertia of the inner housing:

  $J_{x_{CW}} = 0.0016663\,\mathrm{kg\,m^2},\ J_{y_{CW}} = 0.0011666\,\mathrm{kg\,m^2},\ J_{z_{CW}} = 0.0011463\,\mathrm{kg\,m^2}$
- Moments of complete inertia of the outer housing:

  $J_{x_{CZ}} = 0.0003383\,\mathrm{kg\,m^2},\ J_{y_{CZ}} = 0.0002213\,\mathrm{kg\,m^2},\ J_{z_{CZ}} = 0.0002583\,\mathrm{kg\,m^2}$
- Angular velocity of the rotor:

  $n = 600\,\mathrm{rad/s}$
- Friction coefficients in the bearing of the inner and outer housing:

  $c_w = 0.05\,\mathrm{N\,m\,s},\ c_z = 0.05\,\mathrm{N\,m\,s}$
- Maximum torque of the controlling motors:

  $M_{max} = 0.8\,\mathrm{N\,m}$

Figure 3a presents the scope of the air space scanned by the optoelectronic system of the seeker with a large top angle of scanning β_w amounting to 3.84 degrees, while Fig. 3b presents the scope of the scanned space with a small angle of scanning β_w amounting to 0.56 degrees, however β_x, β_y are the constituents of angle $\beta = \beta_w/2$.

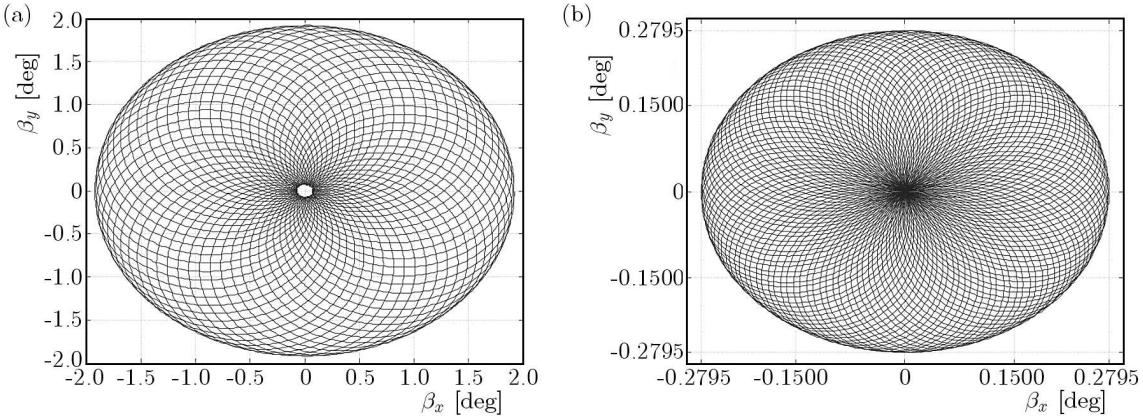

Fig. 3. Scanning of space by the optoelectronic system with a large scanning angle (a) and a small scanning angle (b)

Figure 4 shows the direct detection of the air target by the optoelectronic system moving with the velocity of 200 m/s, which is 3000 m away from the firing position, where X_C, Y_C – coordinates of target location, X_S, Y_S – coordinates of the line of scanning.

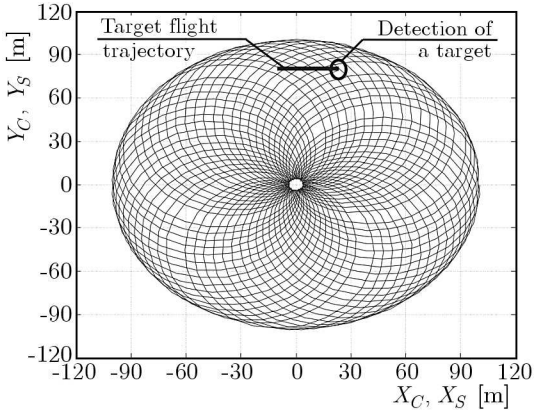

Fig. 4. Direct detection of a target

The time of detecting the target amounted to 0.168 s. The set angular coordinates of the location of the detected target in relation to the seeker axis are as follows: $\sigma = 0.435$ deg, $\varepsilon = 1.5063$ deg.

In the case when the target is outside the area scanned by the optoelectronic system of the device, the optical axis of the seeker is additionally set into programmed motion. It increases the area of searching and, with a suitable selection of velocity of the programmed movement of the seeker axis, gives satisfactorily dense scanning of space.

Controlling the axis of the scanning seeker was checked by setting its movement on the surface of a circular cone and on the surface of the unwinding coil. The parameters of the controller have been chosen according to (Awrejcewicz and Koruba, 2012) and assumed the following values

$$k_w = 100 \qquad k_z = \frac{1}{2}\sqrt{2 + 4k_w} \qquad h_z = \sqrt{2 + 4k_w}$$

Figures 5-9 present the results of computer simulation of the control of the scanning seeker axis setting its movement on the surface of a circular cone at the same time taking into consideration the scanning of the air space by the optoelectronic system of the device. The target was moving with the velocity of 250 m/s and was 3000 m away from the firing position. Figure 5a presents the diagram of the set angular velocity ω_O for the seeker axis moving on the surface of a circular cone. In the initial phase of control, the scanning seeker axis accelerates till the moment of achieving the set angular velocity amounting to 360 deg/s. In the further phase of control, the angular velocity of the axis is maintained at the constant level of 360 deg/s.

Figures 10-14 present the results of computer simulation of the control of the scanning seeker axis setting its movement on the surface of an unwinding spiral at the same time taking into consideration the scanning of the air space by the optoelectronic system of the device. The target was moving with the velocity of 70 m/s and was 3000 m away from the firing position.

Figure 10 presents the diagram of the set angular velocity ω_O for the seeker axis moving on the surface of an unwinding spiral. In the initial phase of control, the axis accelerates till the moment of achieving the set angular velocity amounting to 180 deg/s.

In the further phase of control, the angular velocity of the axis is maintained at the constant level of 180 deg/s.

Figures 12 and 14 present the searching of the air space by the seeker and the detection of the target. In the first of the presented simulations, the time of detecting the target amounted

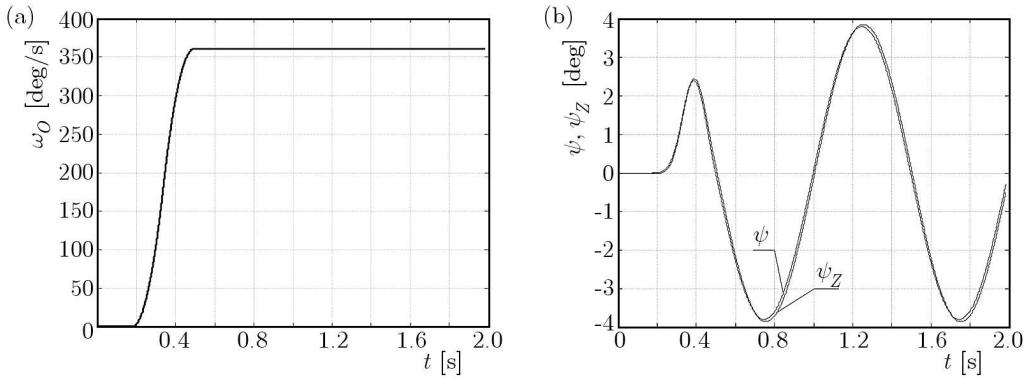

Fig. 5. (a) Set angular velocity of circling around a circular cone by the seeker axis; (b) desired and actual rotation of the outer housing around the axis Z_{CZ}

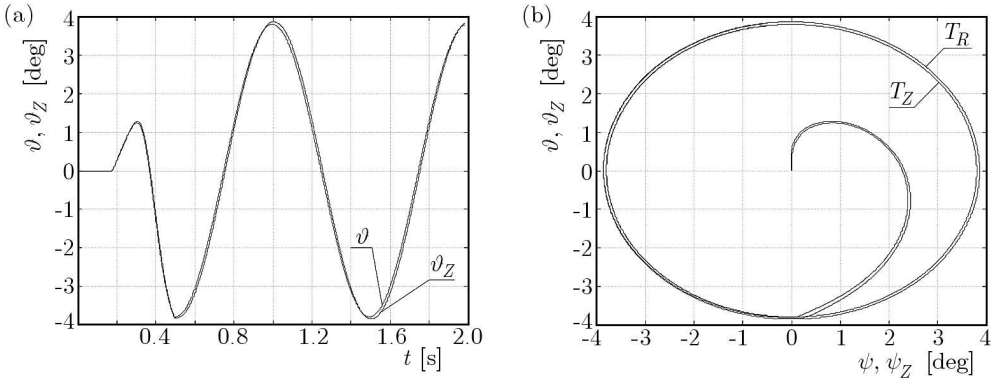

Fig. 6. (a) Desired and actual rotation of the inner housing around the axis X_{CW}; (a) trajectory of the set T_Z and actual T_R movement of the seeker axis

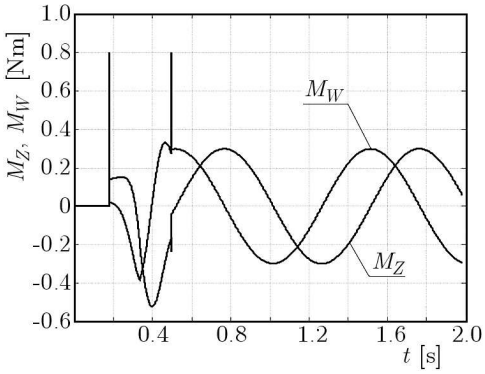

Fig. 7. Moments controlling the outer and inner housing of the seeker

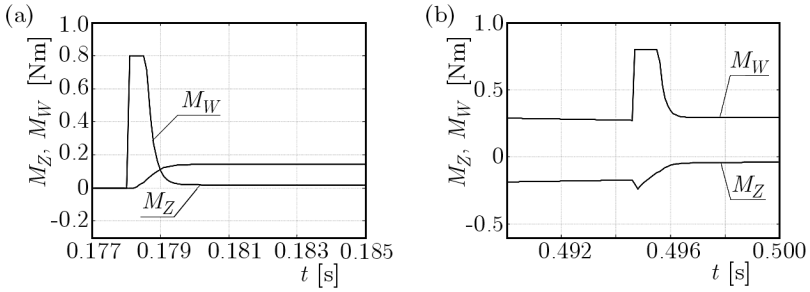

Fig. 8. Controlling moments in transitional periods

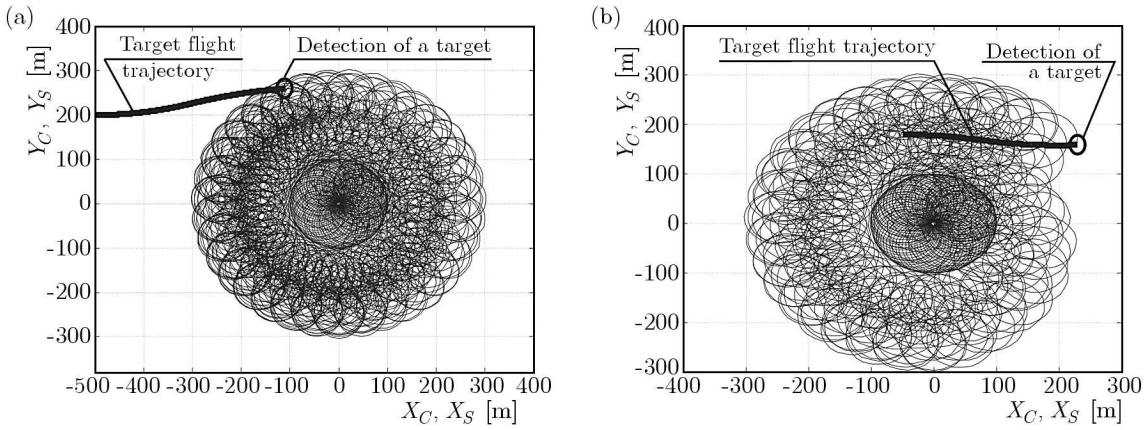

Fig. 9. Searching of the air space by setting the seeker axis into programmed movement on the surface of the circular cone and detecting the air target

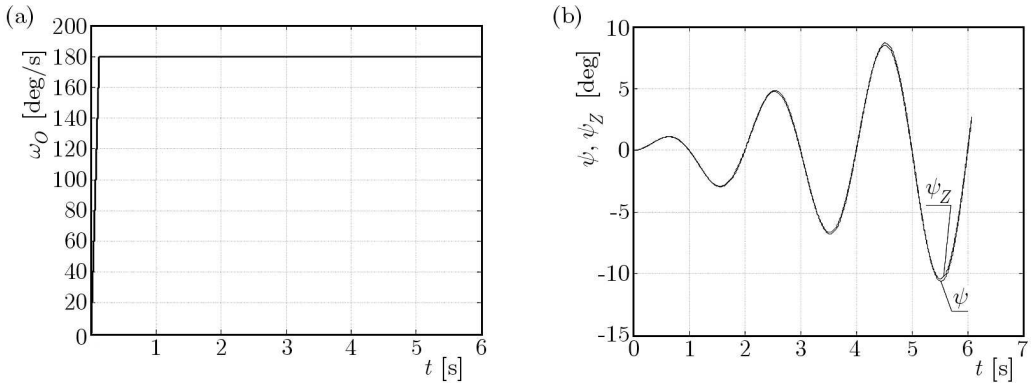

Fig. 10. (a) Set angular velocity of the seeker axis in its movement on the surface of the unwinding spiral; (b) desired and actual rotation of the outer housing around the axis Z_{CZ}

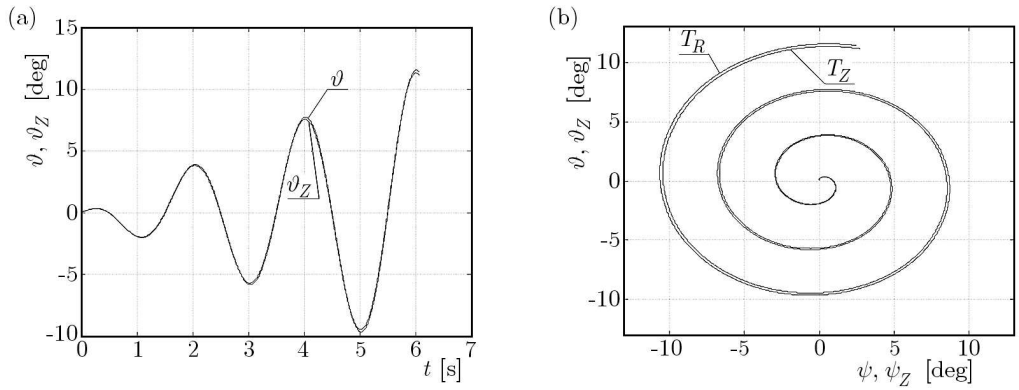

Fig. 11. (a) Desired and actual rotation of the inner housing around the axis X_{CW}; (b) trajectory of the set T_Z and actual T_R movement of the seeker axis

to 6.085 s, while the set angular coordinates of the location of the detected target amounted to: $\sigma = 3.93$ deg, $\varepsilon = 10.192$ deg. In the second case, the time of detecting the target amounted to 5.397 s, while the set angular coordinates of the location of the detected target amounted to: $\sigma = -10.523$ deg, $\varepsilon = -1.88$ deg.

Figures 15 and 16 show the results of computer simulation of controlling the seeker axis by setting it in the first phase in movement on the surface of a circular cone. When the seeker does not detect a target, it passes to the second phase of control on the surface of the unwinding spiral. At the same time, the scanning of the air space by the optoelectronic system of the device

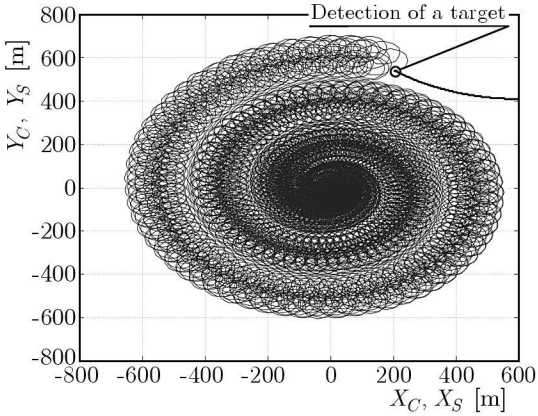

Fig. 12. Searching of the air space by setting the seeker axis into programmed movement on the surface of the unwinding spiral and detecting the air target

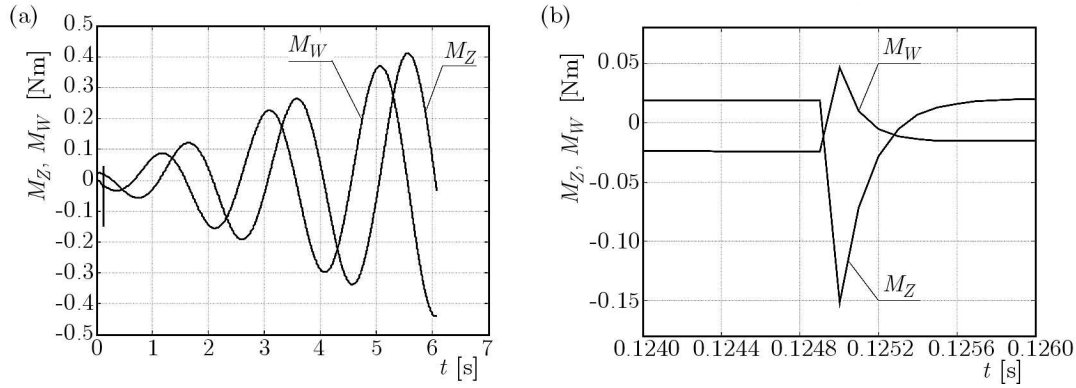

Fig. 13. (a) Moments controlling the outer and inner housing of the seeker; (b) controlling moments in transitional periods

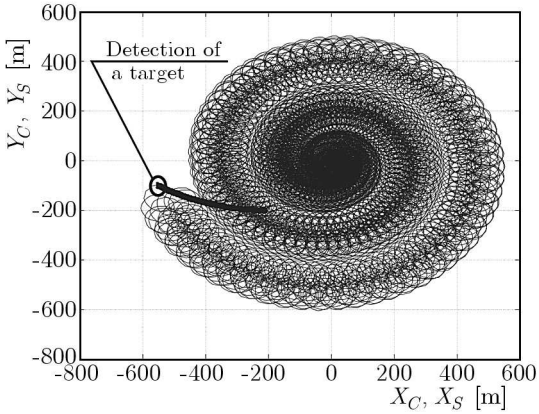

Fig. 14. Searching of the air space by setting the seeker axis into programmed movement on the surface of the unwinding spiral and detecting the air target

was taken into consideration. The target was moving with the velocity of 70 m/s and was 3000 m away from the firing position.

Figure 15a presents the diagram of the set angular velocity ω_O for the seeker axis moving in the first and second phase of control. In the initial phase of control, the scanning seeker axis accelerates till it reaches the set angular velocity amounting to 360 deg/s, which is maintained at a constant level of 360 deg/s until a full circle has been made, after which the second phase of control follows. In the second phase of control, the angular velocity of moving in a spiral decreases till it reaches the set angular velocity amounting to 180 deg/s.

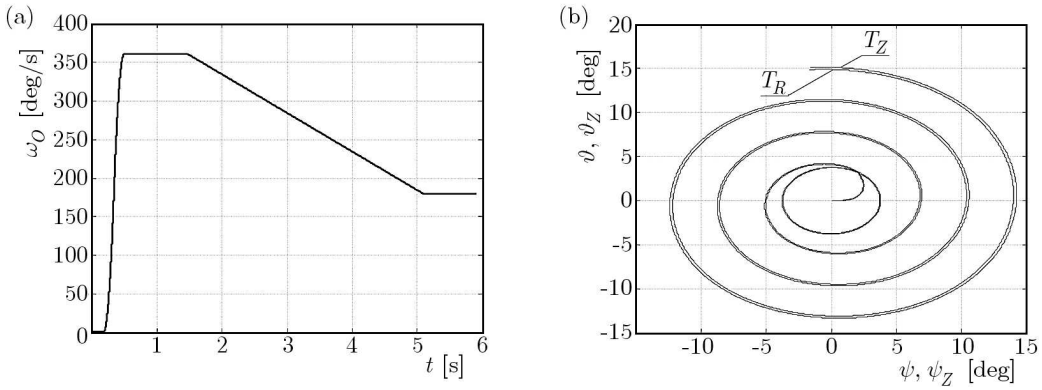

Fig. 15. (a) Set angular velocity of the seeker axis in its movement on the surface of the circular cone and the unwinding spiral; (b) trajectory of the set T_Z and actual T_R movement of the seeker axis

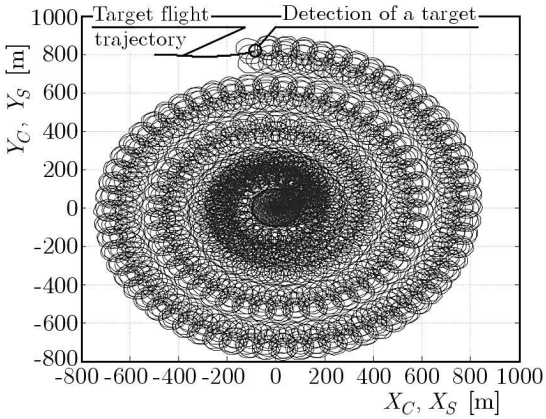

Fig. 16. Searching of the air space by setting the seeker axis into programmed movement and detecting the air target

Figure 16 presents the searching of the air space by the seeker and the detection of the target. The time of detecting the target amounted to 5.9 s. The set angular coordinates of the location of the detected target are as follows: $\sigma = -1.707$ deg, $\varepsilon = 15.137$ deg.

5. Conclusions and final remarks

From the conducted analysis of the dynamics and control of the designed target seeker, it appears that the programmed control of its axis in the phase of searching the air space is done with the precision sufficient for detecting both slowly moving air targets such as helicopters, transport aeroplanes, as well as for detecting targets moving with higher velocities amounting to 1000 km/h. The selection of a suitable trajectory as well as angular velocities of movement of the seeker axis depends, among others, on the type of the air assault means. The searching of the air space in the way presented in Fig. 11b is characterized by a large area of searching the radius of which can exceed even 800 m for the scanned plane that is 3000 m away from the firing position. However, with such a large scanned area, it is possible to successfully detect the target when its velocity does not exceed 300 km/h. Whereas, for the way presented in Fig. 6b, the area of searching is smaller, its radius amounts to 300 m for the scanned plane that is also 3000 m away, however the time of scanning is much shorter due to which it is possible to detect targets moving with higher velocities.

A rocket missile can of course be equipped with a switch enabling one to choose the type of searching of the air space, however on contemporary battlefields, because of quick response time required, the automation of such type of processes is simply unavoidable. The way of searching shown in Fig. 15b, in which the control of the seeker axis is done on the surface of a circular cone, and then when the seeker does not detect any target, it automatically switches to the second phase of control on the surface of the unwinding spiral, can be a suggestion.

Acknowledgements

The work reported herein was undertaken as a part of the research project supported by the National Centre for Research and Development over the period 2011-2014.

References

1. Awrejcewicz J., Koruba Z., 2012, *Classical Mechanics. Applied Mechanics and Mechatronics*, Vol. 30, Springer, New York
2. Baranowski L., 2013, Equations of motion of a spin-stabilized projectile for flight stability testing, *Journal of Theoretical and Applied Mechanics*, **51**, 1, 235-246
3. Barenz J., Kordulla H., Eckhardt R., Kuppel H., Tholl H. D., Baumann R., 2012, Verfahren zum Steuern eines Lenkflugkörpers und Suchkopf für einen Lenkflugkörper, European Patent EP 2466247 A1
4. Blakelock J.H., 1991, *Automatic Control of Aircraft and Missiles*, John Wiley & Sons, New York
5. Gapiński D., 2005, Optical scanning seeker, Patent PL 199721 B1
6. Gapiński D., 2013, Analysis of the optoelectronic system of modified target seeker (in Polish), *Proceedings of 14th Conference ASMOR 2013*, Jastrzębia Góra, Poland, 79-87
7. Koruba Z., Krzysztofik I., Dziopa Z., 2010, An analysis of the gyroscope dynamics of an anti-aircraft missile launched from a mobile platform, *Bulletin of the Polish Academy of Sciences – Technical Sciences*, **58**, 4, 651-656
8. Krzysztofik I., 2012, The dynamics of the controlled observation and tracking head located on a moving vehicle, *Solid State Phenomena*, **180**, 313-322
9. Kröner Ch., 2012, Suchkopf fr einen zielverfolgenden Flugkörper, European Patent EP 2533002 A1
10. Ładyżyńska-Kozdraś E., 2009, The control laws having a form of kinematic relations between deviations in the automatic control of a flying object, *Journal of Theoretical and Applied Mechanics*, **47**, 2, 363-381
11. Moir I., Seabridge A., 2006, *Military Avionics Systems*, John Wiley & Sons Ltd, Chichester
12. Rueger R., Zoz J., 2012, Infrared seeker head, United States Patent US 2012/0248238 A1
13. Shaffer J., 2011, Scanning array for obstacle detection and collision avoidance, United States Patent US 7982662 B2
14. Siouris G. M., 2004, *Missile Guidance and Control Systems*, Springer, New York
15. Wellman W., Borchard J. F., Anderson D., 2010, Optical system for wide field of view staring infrared sensor having improved optical symmetry, European Patent EP 1618358 B1
16. Wild N. R., Leavy P. M., 2012, Optical detection system, United States Patent US RE43681 E
17. Yanushevsky R., 2008, *Modern Missile Guidance*, CRC Press Taylor & Francis Group, New York

Manuscript received September 19, 2013; accepted for print January 21, 2014